metals

MDPI

Article

Microstructure and Dry-Sliding Wear Behavior of B_4C Ceramic Particulate Reinforced Al 5083 Matrix Composite

Qian Zhao [1], Yunhong Liang [1,2,*], Zhihui Zhang [1,3], Xiujuan Li [1] and Luquan Ren [1]

1 The Key Laboratory of Bionic Engineering, Ministry of Education, Jilin University, Changchun 130025, China; zrzhaoqian@163.com (Q.Z.); zhzh@jlu.edu.cn (Z.Z.); xiujuanli@jlu.edu.cn (X.L.); lqren@jlu.edu.cn (L.R.)

2 School of Mechanical, Aerospace and Civil Engineering, University of Manchester, Manchester M139PL, UK

3 State Key Laboratory of Automotive Simulation and Control, Jilin University, Changchun 130025, China

* Correspondence: liangyunhong@jlu.edu.cn; Tel./Fax: +86-431-8509-5760

Academic Editor: Manoj Gupta

Received: 17 August 2016; Accepted: 14 September 2016; Published: 21 September 2016

Abstract: B_4C ceramic particulate–reinforced Al 5083 matrix composite with various B_4C content was fabricated successfully via hot-press sintering under Argon atmosphere. B_4C particles presented relative high wettability, bonding strength and symmetrical distribution in the Al 5083 matrix. The hardness value, friction coefficient and wear resistance of the composite were higher than those of the Al 5083 matrix. The augment of the B_4C content resulted in the increase of the friction coefficient and decrease of the wear mass loss, respectively. The 30 wt % B_4C/Al 5083 composite exhibited the highest wear resistance. At a low load of 50 N, the dominant wear mechanisms of the B_4C/Al 5083 composite were micro-cutting and abrasive wear. At a high load of 200 N, the dominant wear mechanisms were micro-cutting and adhesion wear associated with the formation of the delamination layer which protected the composite from further wear and enhanced the wear resistance under the condition of high load.

Keywords: aluminum matrix composite; hot pressed sintering; ceramic; wear

1. Introduction

Due to the combination properties of high strength, hardness and wear resistance [1] in modern technology, metal matrix composites (MMCs) have many potential applications in the aerospace, automobile and marine industries [2,3]. Owing to the characteristics of low density, easy workability and high mechanical properties, aluminum alloy is treated as a kind of matrix material in ceramic-reinforced metal matrix composites [4]. As one kind of the most widely used aluminum alloys, the properties of high corrosion resistance, weldability and strength result in the wide use of Al 5083 in practical applications. Because of the potential for good wear resistance, it is worthy to develop the Al 5083 matrix composite.

Among various ceramic particulates used as reinforcement, B_4C is an attractive reinforcement material because of its good chemical and thermal stability, lower density and higher elastic modulus [5–8], which make it the best candidate for the reinforcement of the Al 5083 composite. Moreover, B_4C has excellent mechanical properties such as high hardness and wear resistance [9], which increase its practicability in the Al matrix composite. The incorporation of B_4C and Al alloy provides good physical and mechanical properties [10], in the way of combining the toughness of the Al alloy 5083 with the hardness of the B_4C ceramic particulate to improve the wear resistance of the B_4C ceramic particulate–reinforced Al 5083 composite.

Much research has been done on the fabrication, mechanical properties and wear resistance of ceramic-reinforced Al matrix composites. Wu and co-workers [11] investigated the influence of

plasma-activated sintering parameters on the microstructure and mechanical properties of Al-7075/B_4C matrix composite. They found that the B_4C/Al 7075 composite sintered at 530 °C for 3 min exhibited high mechanical properties including hardness, bending strength, compression yield strength and fracture strength. Ipek et al. [12] studied the wear characteristics of 4147 Al/B_4C with 10, 15 and 20 wt % B_4C particles by adding some kinds of additives (C, B, TiB_2 and SiC). The results showed that the wear resistance of the Al/B_4C matrix increased considerably with the increase of the B_4C content in the Al alloy matrix. The main wear mechanism in this study was adhesive wear. After studying the effect of sliding time, applied load, sliding velocity and heat treatment on friction and wear behaviors of the B_4C/6061Al composite, Dou and co-workers [13] found that under the condition of critical values of sliding time, applied load and sliding velocity, the wear mass loss and friction coefficient increased significantly. These investigations about the wear behavior of the Al matrix composite promoted the practical application of the aluminum matrix composite in anti-wear field.

Up until now, many kinds of methods have been used to fabricate ceramic-reinforced Al matrix composite, such as the stirring casting technique [14], the melt infiltration process [15], plasma spraying [16] and so on. Though the composite fabricated by these methods possesses a relatively high anti-wear property, the limitations of conversion cost and mechanical properties limit the practical applications. Moreover, because of the characteristics of B_4C, monolithic boron carbide cannot be sintered to obtain satisfactory densities without applied pressure even at temperatures over 2280 °C [17]. Kang et al. [18] fabricated a series of B_4C matrix composites with different contents of Al which were synthesized by reaction hot-press sintering with milled B_4C and pure metallic Al powder at 1600 °C for 1 h. Arslan and co-workers [19] found that B_4C/Al composites were composed of various combinations of Al_3BC, AlB_2, $AlB_{12}C_2$ and Al_4C_3, during the reaction process between B_4C and Al. Halverson et al. [20] reported that the reactions in the B_4C/Al composite fabricated by hot-press sintering were the driving force for the wetting of B_4C by molten aluminum, which enhanced the compactness and strength of the B_4C/Al composite. Compared with the other fabrication techniques, the technique considering wear resistance, efficiency and energy conservation, hot-press sintering provides a suitable method to fabricate a ceramic-reinforced Al matrix composite with high compactness, strength and wear resistance. The investigation and analysis on the fabrication methods, especially the hot-press sintering of B_4C-reinforced Al matrix composite, provide the feasibility for the B_4C ceramic–reinforced Al 5083 matrix composite, in which the composites are reinforced by the relatively larger amount of particles to achieve higher wear resistance, higher toughness and strength.

In this paper, B_4C/Al 5083 composites with various B_4C contents were fabricated via the method of hot-press sintering. Besides the metallographic phase and phase component, the effect of the B_4C content on the wear resistance of the B_4C/Al 5083 composite has also been studied. The experimental results are expected to significantly help develop and prompt the practical application of anti-wear techniques of ceramic particulate–reinforced aluminum alloy composites.

2. Experimental Details

2.1. Material

The starting materials were made from commercial powders of Al 5083 aluminum (99.5% purity ~48 μm) and boron carbide (99.9% purity ~13 μm). Al 5083 powders mixed with 10–30 wt % B_4C contents were used for the powder blends. In order to remove the impurities in B_4C and Al 5083 powders, B_4C and Al 5083 particles were heated to 450 °C and 250 °C for 1 h, respectively. The B_4C and Al 5083 powders were mixed in a stainless steel container using stainless-steel balls at a low speed (~35 rpm) for 8 h to ensure homogeneity, and then pressed into cylindrical compacts (about 45 mm in diameter and 20 ± 2 mm in length) using a stainless steel die to obtain densities of 65% ± 2% theoretical density. After being dried in a vacuum oven at about 100 °C for 3 h to remove any trace of moisture, the compacts with various B_4C contents were placed on the bottom of a graphite die. Then the graphite die with compact was put into a self-made vacuum thermal explosion furnace under

Argon atmosphere. All of the cylindrical compacts were heated to 650 °C to melt Al 5083 matrix and initiate reaction between B_4C ceramic particles and Al 5083 matrix. During heating process the temperature of graphite die was measured by an infrared temperature measuring sensor (Asmik, Hangzhou, China). After maintaining the temperature for 10 min at 650 °C, the temperature of graphite die was decreased to the melting point of Al 5083 and in the process of the 10 min. Then the pressure of 3 t was applied on graphite die to increase density of B_4C/Al 5083 composite. After keeping the pressure for 5 min and then cooling the sample down, the composite was ready for metallographic and wear experiments. In order to exhibit changes in wear resistance of B_4C/Al 5083 composite, the pure Al 5083 matrix was fabricated under the same preparation conditions.

2.2. Metallographic Experiment

Metallographic sample with dimension of 10 mm × 10 mm × 10 mm (Length × Width × Thickness) was prepared by a wire-electrode cutting machine (Huawei CNC Machine Tool Manufacture Co. Ltd., Taizhou, China) to carry out metallography experiment. The samples were polished to get a smooth surface and etched by Keller's reagent (1 vol. % HF + 1.5 vol. % HCl + 2.5 vol. % HNO_3 + 95 vol. % H_2O). After ultrasonically clean in alcohol for 10 min, the specimens were dried in hot air to obtain a clean surface.

2.3. Wear Test

The hardness of samples was measured according to the Brinell hardness tester (MHBD-3000P, Shanghai Jujing Precision Instrument Manufacturing Co., Ltd., Shanghai, China) by applying a load of 100 g for 5 s. The average value of the hardness was obtained from six individual measurements.

After hardness test, the dry-sliding wear test was conducted using a high-temperature friction and wear tester (Model MG-2000, Xuanhua Kehua Testing Machine Manufacturing Co., Ltd., Zhangjiakou, China) in a pin-on-disk contact configuration at room temperature of about 26 °C and relative humidity of 30%. The B_4C/Al 5083 composite was cut into cylindrical pins with dimension of Φ6 mm × 15 mm by wire-electrode cutting machine (Huawei CNC Machine Tool Manufacture Co. Ltd., Taizhou, China). The disk with dimension of Φ70 mm × 15 mm was made of 4Cr5MoSiV1 (AISI H13) with hardness of 50 ± 1 HRC and surface roughness of Ra = 0.8 μm. The pins were grounded to get the smooth surface. Both pins and discs were ultrasonically cleaned in ethyl alcohol for 10 min and then dried in hot air to remove the rust and obtain clean surface. The pin was loaded against the disk with a dead-weight loading system. To investigate the effect of different loads on the wear morphology and mechanism of B_4C/Al 5083 composite, the friction and wear experiments were conducted at the loads of 50 N, 100 N, 150 N and 200 N (at a constant rotation rate of 200 rpm and wear time of 10 min), respectively. The friction coefficient can be recorded automatically by the software (Xuanhua Kehua Testing Machine Manufacturing Co., Ltd., Zhangjiakou, China) of wear tester. An electronic balance with the precision of 0.01 mg was used to weight the wear mass loss, which was applied to assess the anti-wear property. The average value of the three parallel test results was calculated.

In order to investigate the wear mechanism of B_4C/Al 5083 composite, the metallographic phase, microstructure and wear surface of composite were examined using scanning electron microscopy (SEM) (Model Evo18, Carl Zeiss, Oberkochen, Germany) together with energy-dispersive spectrometry (EDS) (Model Oxford Instruments, Oxford, UK). The phase components were identified using X-ray diffraction (XRD) (Model D/Max 2500PC, Rigaku, Tokyo, Japan).

3. Results and Discussion

3.1. Microstructure and Phase Composition of B_4C/Al 5083 Composite

B_4C/Al 5083 composites with 10–30 wt % B_4C contents were successfully fabricated using the hot-press sintering method under Argon atmosphere. As shown in Figure 1, the B_4C/Al 5083 composite

exhibits a relatively higher compactness. Only a few pores can be observed in the local region, which reflects the advantage of hot-press sintering and builds the base of high wear resistance.

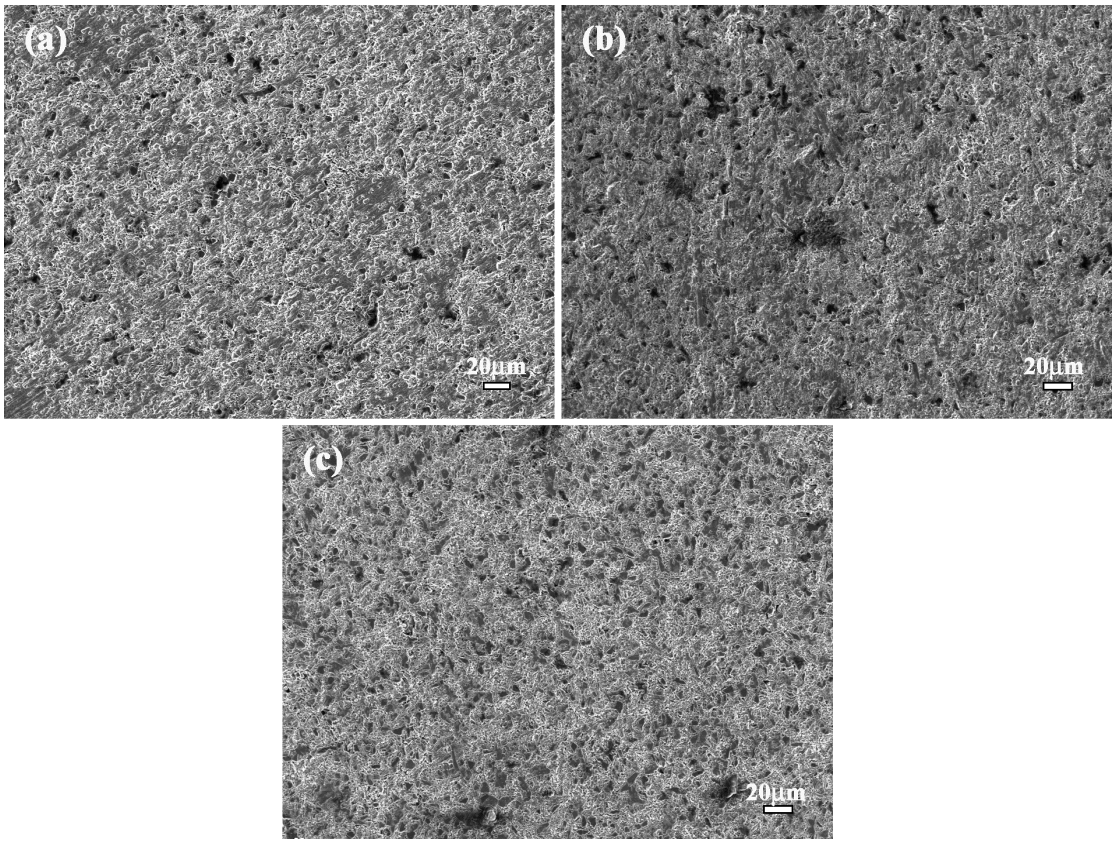

Figure 1. Compactness of B_4C/Al 5083 composite with (**a**) 10 wt % B_4C content; (**b**) 20 wt % B_4C content; (**c**) 30 wt % B_4C content.

The metallography of the B_4C/Al 5083 composite with 10 wt % and 30 wt % B_4C content is given in Figure 2a,b, respectively. Variation of the B_4C content has a significant effect on the corresponding metallography of the composite. B_4C particles present a relatively symmetrical distribution in the Al 5083 matrix. No accumulation and macro-segregation phenomena exist in the B_4C/Al 5083 composite. The fracture morphologies and corresponding EDS analysis of 10–30 wt % B_4C/Al 5083 composite are shown in Figure 3. After the operation of mechanical fracture, the pits resulting from the extraction of B_4C exist on the fracture surface. B_4C with a similar particle size presents a uniform distribution in the Al 5083 matrix. Variation of the B_4C significantly affects the fracture morphology. With the increase of the B_4C content, the number of pits increases clearly. Moreover, the B_4C particles show a high bonding strength with the Al 5083 matrix, which exhibits the high wettability of B_4C. The EDS analysis of 30 wt % B_4C/Al 5083 composite indicates that the elements in the line scanning area of Figure 3c consist of B, C, O, Mg, Al and Si. The weight percentages of B, C, O, Mg, Al and Si are 74.84, 11.32, 1.66, 0.28, 11.87 and 0.04 wt %, respectively. The atom percentages of B, C, O, Mg, Al and Si are 82.2, 11.19, 1.23, 0.14, 5.22 and 0.22 at %, respectively. The existence of Mg and Si results from the components of Al 5083. The appearance, high weight percentage and atom percentage of B and C confirm the existence and position of B_4C. Metallography, fracture and EDS results approve the existence of B_4C ceramic particles from the point view of the microstructure. Moreover, metallurgical bonding between ceramics and the Al 5083 matrix and the uniform ceramic particle size and distribution reveal the feasibility and superiority of the hot-press sintering method.

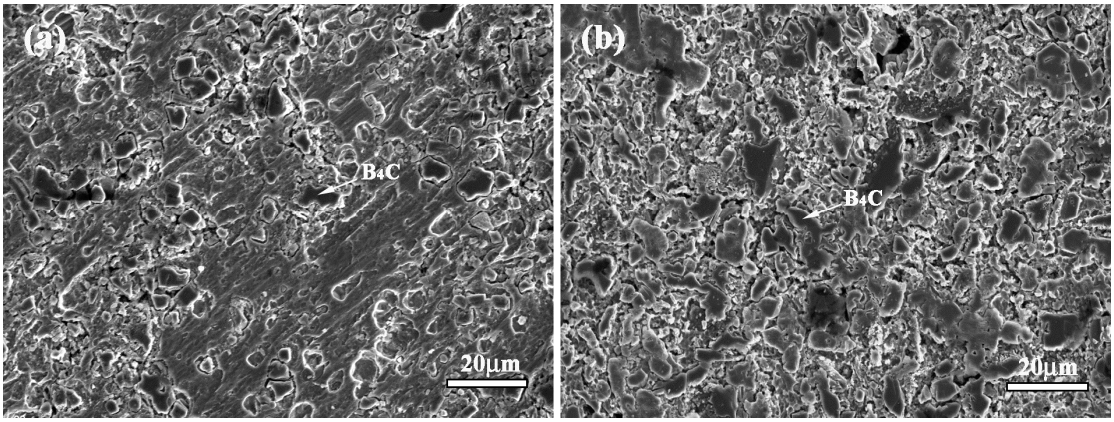

Figure 2. Metallography of B_4C/Al 5083 composite with (**a**) 10 wt % B_4C content and (**b**) 30 wt % B_4C content.

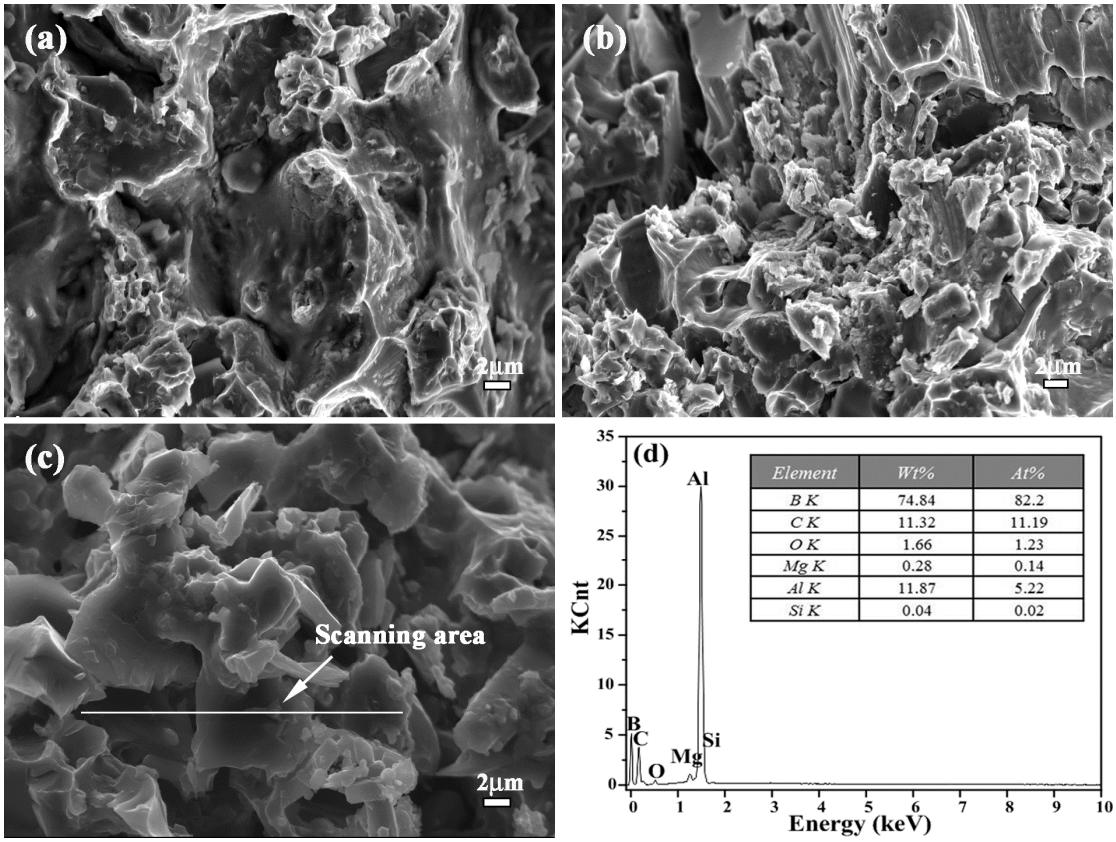

Figure 3. Fracture morphology of B_4C/Al 5083 composite with (**a**) 10 wt % B_4C content; (**b**) 20 wt % B_4C content; (**c**) 30 wt % B_4C content; (**d**) EDS analysis of (**c**).

Figure 4 show the phase identification of the B_4C/Al 5083 composite with 10–30 wt % B_4C contents. As indicated, besides Al and B_4C, the B_4C/Al 5083 composite consists of $B_{13}C_2$, $A_{l3}BC$, Al_4C_3 and Al_2O_3, as shown in Figure 4a–c. The phase of Al_2O_3 results from the pretreatment of Al 5083 at 250 °C. Part of the Al 5083 reacts with oxygen, which corresponds to the element of O in Figure 3c. Halverson and co-workers [20] declared the reaction behavior between B_4C and the Al matrix in detail. In the hot-press sintering process, B_4C reacted with Al 5083, forming the $B_{13}C_2$, $A_{l3}BC$ and Al_4C_3. The elements that exist in the products are similar to the EDS results in Figure 3d. These interfacial reactions are considered as the driving force to enhance the wettability of B_4C in the Al 5083 matrix.

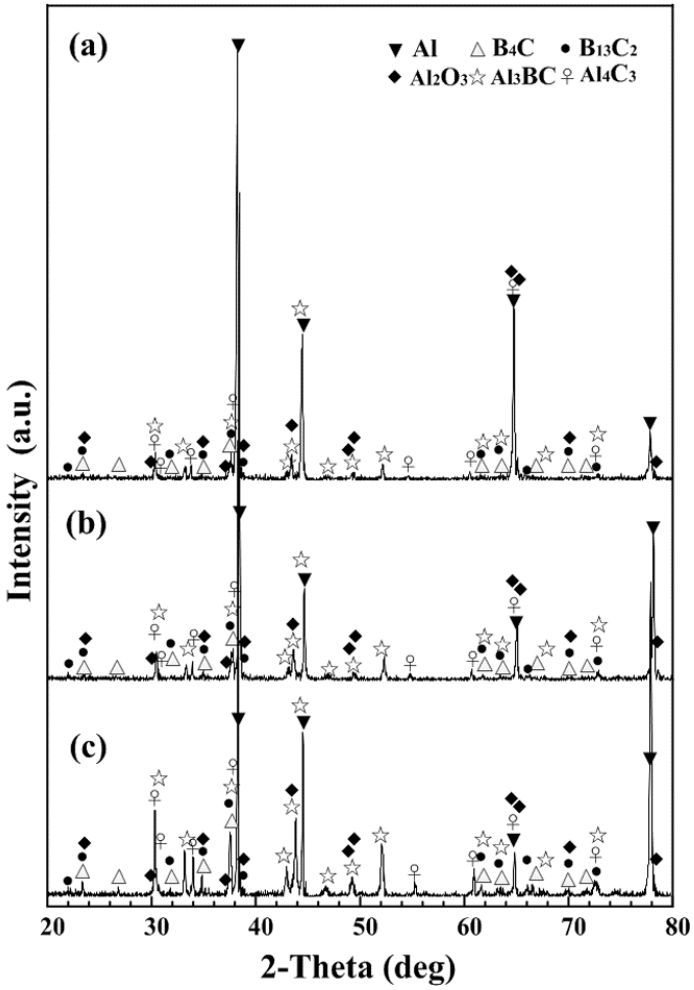

Figure 4. Phase identification of B_4C/Al 5083 composite with (**a**) 10 wt % B_4C content; (**b**) 20 wt % B_4C content; (**c**) 30 wt % B_4C content.

The result of Figure 4 confirms the existence of B_4C in the reacted B_4C/Al 5083 composite from the point view of phase identification. Based on Figures 1–4, the B_4C-reinforced Al 5083 matrix composite was fabricated successfully by hot-press sintering under Argon atmosphere. The steady phase components play an important role in bonding strength and wear resistance. Therefore, based on the characteristics of microstructure and phase components, the wear resistance of the B_4C/Al 5083 composite was investigated.

3.2. Hardness

Microhardness values of the pure Al 5083 matrix and 10–30 wt % B_4C/Al 5083 composite are shown in Figure 5. Al 5083 matrix owns the minimal hardness value (45.7 HB). The microhardness values of 10–30 wt % B_4C/Al 5083 composites are 48.5 HB, 66.7 HB and 110.5 HB, respectively. When the B_4C content increases from 10 wt % to 30 wt %, the hardness value increases gradually, which can be attributed to the increase of the ceramic content.

Wear resistance of the composites is influenced by many factors such as the ceramic content, hardness value, interface bonding and so on. Variation of the B_4C content significantly affects the microstructure and hardness of the B_4C/Al 5083 composite. In order to investigate the influence of the B_4C content on the wear resistance property and wear mechanism of the B_4C/Al 5083 composite, dry-sliding wear tests with different loads were conducted.

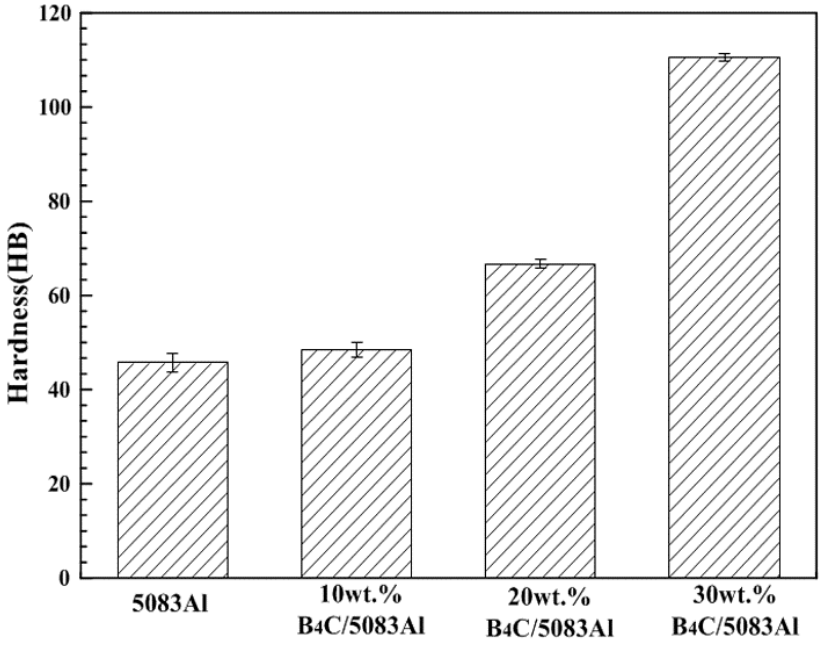

Figure 5. Microhardness of pure Al 5083 matrix and B_4C/Al 5083 composite with 10–30 wt % B_4C content.

3.3. Wear Behavior

Figure 6a shows the variation of the friction coefficient of the Al 5083 matrix and 10–30 wt % B_4C/Al 5083 composite varying with applied load at a rotation rate of 200 rpm, respectively. From Figure 6a it can be found that the friction coefficients of B_4C/Al 5083 composites are higher than that of the Al 5083 matrix, and the friction coefficients of all composites are in the range of 0.40–0.60. With the increase of the B_4C content, the friction coefficient of the B_4C/Al 5083 composite increases measurably. Figure 6b shows the wear mass loss of the Al 5083 matrix and 10–30 wt % B_4C/Al 5083 composite varying with applied load. From Figure 6b it can be seen that the wear mass loss of the B_4C/Al 5083 composites is lower than that of the Al 5083 matrix, which indicates the higher wear resistance of the B_4C/Al 5083 composite. Moreover, the composite with 30 wt % B_4C content shows the best anti-wear property. With the increase of the B_4C content, the wear mass loss increases monotonously, which means that the B_4C content significantly affects the wear resistance of the composite.

Hardness was the key point for enhancing the wear resistance of the B_4C/Al 5083 composite. The existence of B_4C particles significantly strengthened the hardness of the composite, resulting in the low wear mass loss of the composite, as shown in Figure 6b. With the increase of the B_4C content, the wear mass loss of the composites increased, which can be owed to the combination of hardness and metallurgy bonding between reinforcements and the Al 5083 matrix. With the increase of the B_4C content, the contact area between the reinforcement and Al 5083 matrix increased, the interface reactions between B_4C and Al 5083 maintained the high bonding strength of the composites. B_4C played the load-bearing role during the dry-sliding process. The absence of reinforcement resulted in the highest wear mass loss of the Al 5083 matrix. During the wear process the high amount of B_4C content resulted in high hardness, which led to the lowest wear mass loss of the composite with 30 wt % B_4C. The existence of pores decreased the bonding strength of B_4C in the composites. After the wear experiment was conducted for a moment, the Al 5083 that was around the ceramic particulates wore out firstly, leading to the decrease of the real contact area and the adhesion between counterparts. The wear model was changed from sliding wear to rolling wear by the desquamated B_4C particles which are around the pores. The decrease of the real contact area, adhesion and the change of wear

model resulted in the decrease of friction force and increased the friction coefficient, as shown in Figure 6a. The strong bonding and high hardness value led to the lesser amount of desquamated ceramic, resulting in the highest friction coefficient of the 30 wt % B_4C/Al 5083 composite.

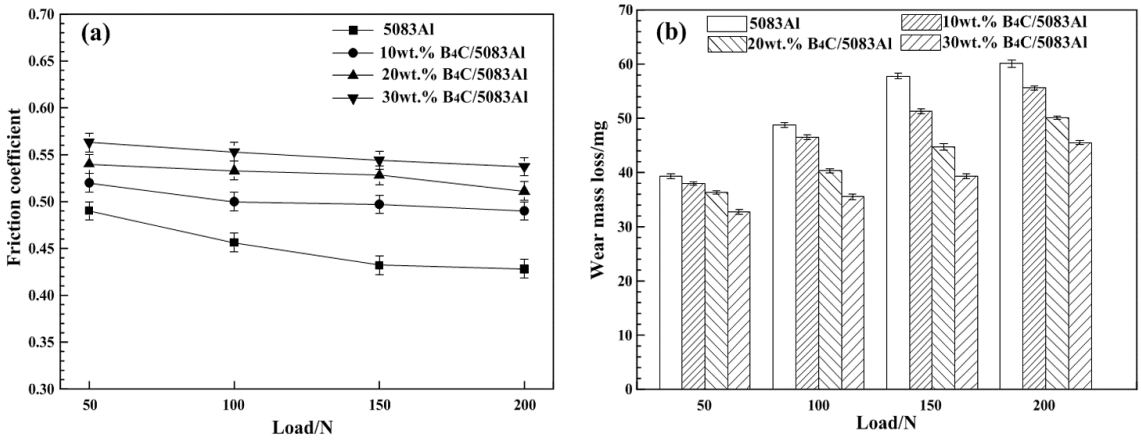

Figure 6. (**a**) Friction coefficient and (**b**) wear mass loss of Al matrix and B_4C/Al 5083 composite under different applied loads.

3.4. Wear Surface

Figure 7a–h exhibit the SEM micrographs and the corresponding magnified morphology of the worn surfaces of the Al 5083 matrix and B_4C/Al 5083 composites at the low load of 50 N, respectively. Compared with the Al 5083 matrix, the B_4C/Al 5083 composites show lighter scratch severity. At the low load of 50 N, the worn surfaces of the composites are characterized by a lot of long continuous grooves and wear debris. The magnified morphology expresses the wear mechanism of the B_4C/Al 5083 composite at low applied load further. The large amount of granular wear debris and grooves declare that the dominant wear mechanisms are micro-cutting and abrasive wear, as shown in Figure 7d,f,h.

When the applied load increases to 200 N, besides grooves and granular wear debris, many delamination layers adhere on the worn surfaces, as shown in Figure 8a,c,e,g. At the applied load of 200 N, the deformation of the worn surface of B_4C/Al 5083 composites indicates the presence of serious wear progress. The magnified morphology of the worn surfaces of B_4C/Al 5083 composites, as shown in Figure 8d,f,h, exhibits the characteristic of a large amount of granular wear debris under the applied loads of 200 N, which is similar to that at 50 N. Compared with the magnified micrographs at 50 N, typical forms of grooves and delamination layers on worn surfaces illustrate the dominant wear mechanisms of micro-cutting and adhesive wear at a high applied load of 200 N. The relative slight delamination layer phenomenon of the 30 wt % B_4C/Al 5083 composite shows the relatively higher wear resistance, which is similar to the result in Figure 6a.

The contact characteristics between the pin and disc were changed by the existence of the hard reinforcement of B_4C. Due to the hardness disparity between the reinforcement and matrix, the Al 5083 matrix was worn out firstly. During the wear process, wear debris were removed and pushed into the ridges along the sides of the sliding direction, which forms the appearance of grooves. The deficiency of the Al 5083 matrix enhanced the load-bearing role of the B_4C ceramic particulates and increased its desquamation possibility. The desquamated B_4C and Al 5083 matrix changed the wear behaviors and formed the dominant wear mechanism of abrasive wear. With the increase of the applied load, the dominant wear mechanism of the B_4C/Al 5083 composite changed from abrasive wear to adhesion wear. In the wear system composed by the pin and disc, the Al 5083 matrix was desquamated by the shear stress, resulting in the plastic deformation of the B_4C/Al 5083 composite periodically. Stress concentration resulting from the plastic deformation between the pin and disc

led to the delamination layer phenomenon of adhesion wear, which protected the composite from further friction and enhanced the wear resistance of the B_4C/Al 5083 composite, as shown in Figure 8. Considering of the economy, efficiency and high wear resistance, the B_4C/Al 5083 composite fabricated via the hot-press sintering route can be widely used in practical applications of the wear resistance field.

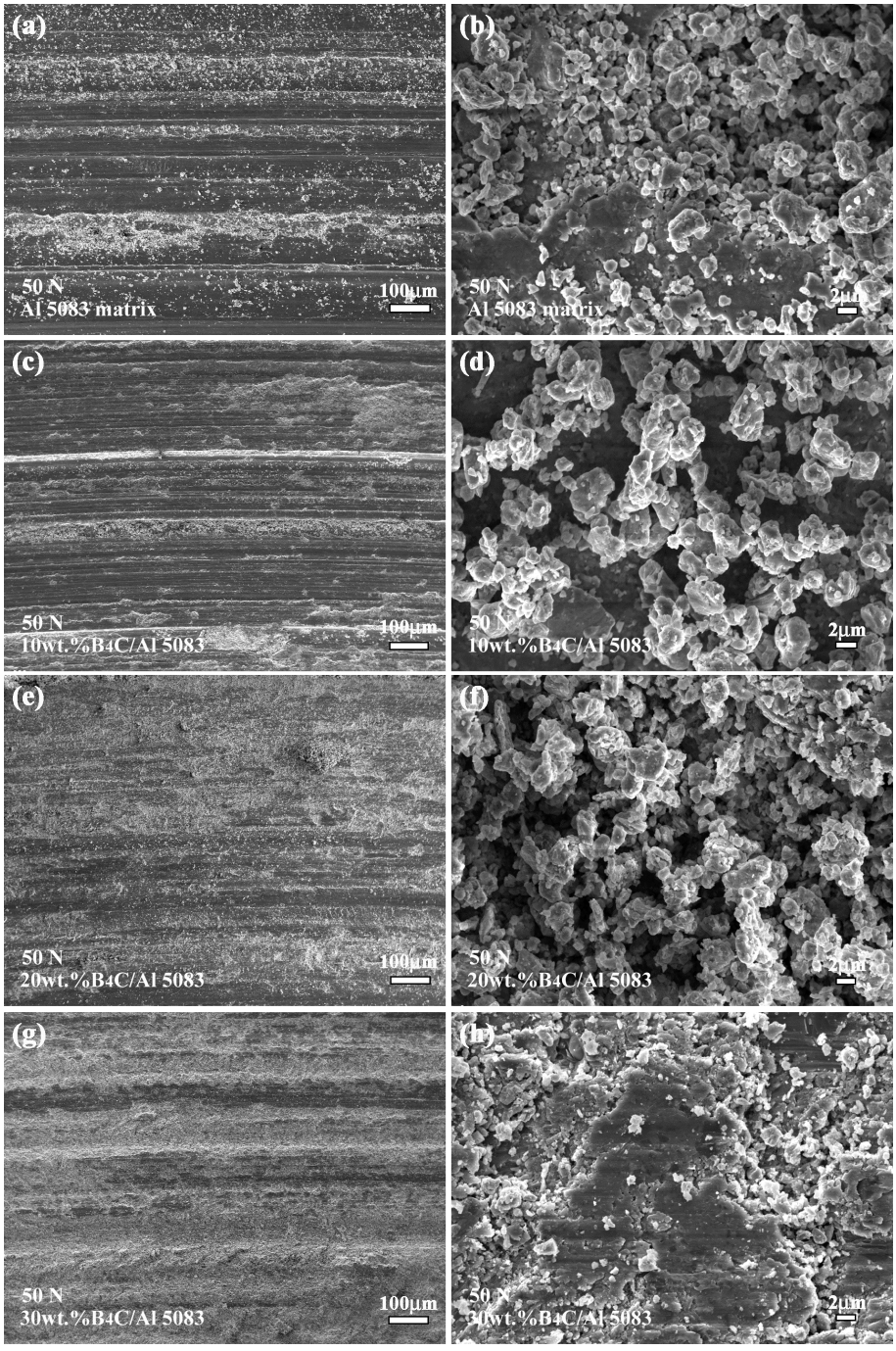

Figure 7. Worn surface of (**a**) Al 5083 matrix at 50 N; (**b**) magnified morphology of (**a**); (**c**) 10 wt % B_4C/Al 5083 composite at 50 N; (**d**) magnified morphology of (**c**); (**e**) 20 wt % B_4C/Al 5083 composite at 50 N; (**f**) magnified morphology of (**e**); (**g**) 30 wt % B_4C/Al 5083 composite at 50 N and (**h**) magnified morphology of (**g**).

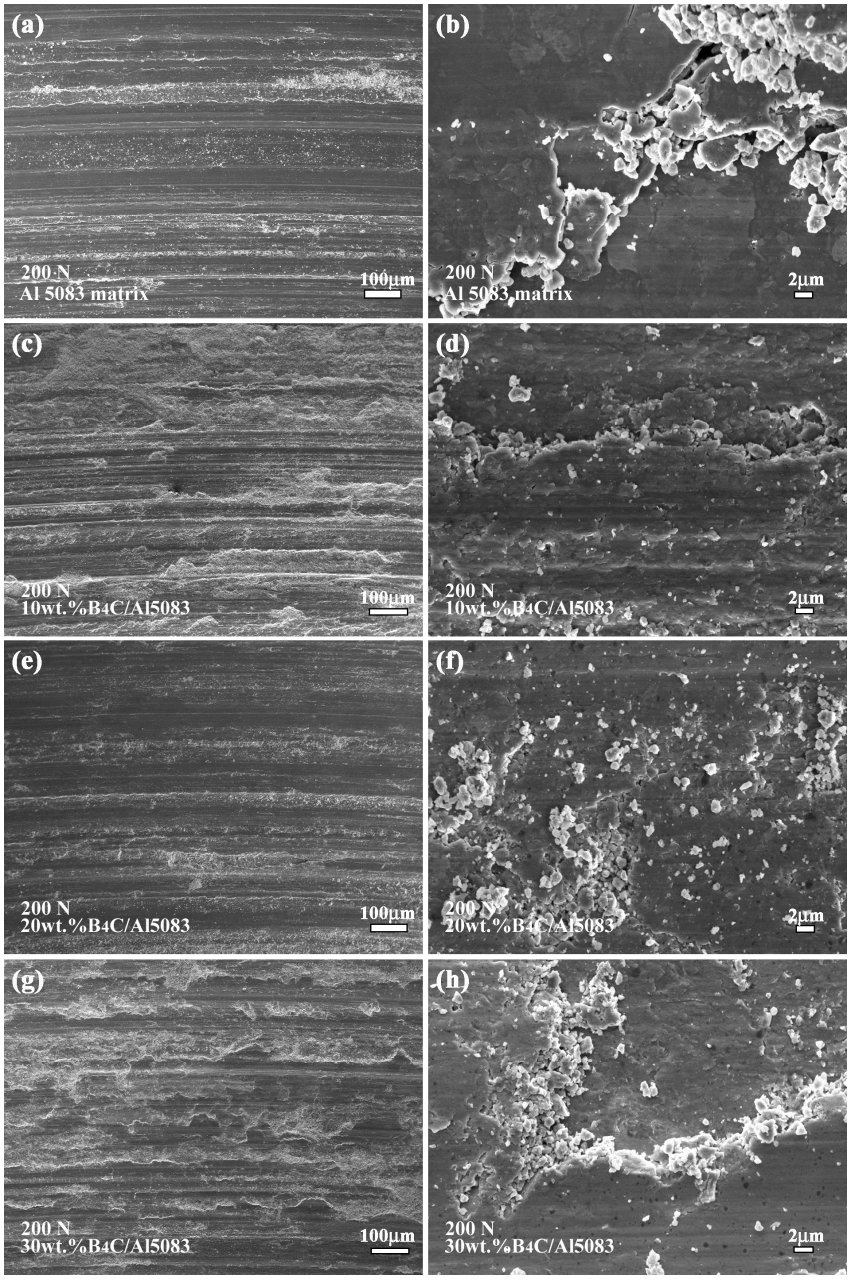

Figure 8. Worn surface of (**a**) Al 5083 matrix at 200 N; (**b**) magnified morphology of (**a**); (**c**) 10 wt % B_4C/Al 5083 composite at 200 N; (**d**) magnified morphology of (**c**); (**e**) 20 wt % B_4C/Al 5083 composite at 200 N; (**f**) magnified morphology of (**e**); (**g**) 30 wt % B_4C/Al 5083 composite at 200 N and (**h**) magnified morphology of (**g**).

4. Conclusions

In this study, the microstructure, phase component and wear mechanism of B_4C ceramic particulate–reinforced Al 5083 composites with various B_4C contents fabricated via a hot-press sintering route were studied. The conclusions are described as follows:

(1) A B_4C/Al 5083 composite with a relatively higher density was fabricated successfully. B_4C particles presented a relatively homogeneous distribution in the Al 5083 matrix. No severe particle segregation phenomenon existed in the composite.

(2) The $B_{13}C2$, Al_3BC and Al_4C_3 phases were detected from XRD patterns, suggesting B_4C particles have reacted with the Al5083 matrix, which enhanced the wettability of the B_4C in the matrix.

(3) The hardness values, friction coefficient and wear resistance of the B_4C/Al 5083 composites were higher than those of the Al 5083 matrix. The 30 wt % B_4C/Al 5083 composite exhibited the highest wear resistance and friction coefficient.

(4) At a low applied load of 50 N, the dominant wear mechanisms of the B_4C/Al 5083 composites were micro-cutting and abrasive wear. At a high load of 200 N, the dominant wear mechanisms were micro-cutting and adhesion wear. The adhesion wear was associated with the formation of a delamination layer, which protected the composite from further wear and enhanced the wear resistance.

Acknowledgments: This work is supported by Cooperative Innovation Platform of National Oil Shale Exploration Development and Research, the National Natural Science Foundation (No. 51675223 and 51375006), National Major Scientific Instruments and Equipment Development Projects (2012YQ030075-09-04).

Author Contributions: Yunhong Liang, Luquan Ren and Qian Zhao conceived and designed the experiments; Qian Zhao performed the experiments; Zhihui Zhang and Qian Zhao analyzed the data; Xiujuan Li contributed reagents, materials and analysis tools; Qian Zhao wrote the paper.

Conflicts of Interest: The authors declare no conflict of interest.

References

1. Toptan, F.; Kilicarslan, A.; Kertil, I. The effect of Ti addition on the properties of Al-B_4C interface: A microstructural study. *Mater. Sci. Forum* **2010**, *636*, 192–197. [CrossRef]
2. Zhang, Z.; Zhang, J.; Mai, Y. Wear behavior of SiC_p/Al-Si composites. *Wear* **1994**, *176*, 231–237.
3. Alizadeh, A.; Abdollahi, L.; Biukani, H. Creep behavior and wear resistance of Al 5083 based hybrid composites reinforced with carbon nanotubes (CNTs) and boron carbide (B_4C). *J. Alloy. Compd.* **2015**, *650*, 783–793. [CrossRef]
4. Baradeswaran, A.; Perumal, A.E. Influence of B_4C on the tribological and mechanical properties of Al 7075-B_4C composites. *Compos. B-Eng.* **2013**, *54*, 146–152. [CrossRef]
5. Aizenshtein, M.; Froumin, N.; Shapiro, T.E.; Dariel, M.P.; Frage, N. Wetting and interface phenomena in the B_4C/(Cu-B-Si) system. *Scr. Mater.* **2005**, *53*, 1231–1235. [CrossRef]
6. Jung, J.; Kang, S. Advances in manufacturing boron carbide-aluminum composites. *J. Am. Ceram. Soc.* **2004**, *87*, 47–54. [CrossRef]
7. Zhu, X.; Dong, H.; Lu, K. Coating different thickness nickel-boron nanolayers onto boroncarbide particles. *Surf. Coat. Technol.* **2008**, *202*, 2927–2934. [CrossRef]
8. Shrestha, N.K.; Kawai, M.; Saji, T. Co-deposition of B_4C particles and nickel under the influence of a redox-active surfactant and anti-wear property of the coatings. *Surf. Coat. Technol.* **2005**, *200*, 2414–2419. [CrossRef]
9. Johnson, W.C. Advanced materials and powders. *Am. Ceram. Soc. Bull.* **2001**, *80*, 64–66.
10. Shen, Q.; Wu, C.D.; Luo, G.Q.; Fang, P.; Li, C.Z.; Wang, Y.Y.; Zhang, L.M. Microstructure and mechanical properties of Al-7075/B_4C composites fabricated by plasma activated sintering. *J. Alloy. Compd.* **2014**, *588*, 265–270. [CrossRef]
11. Wu, C.D.; Fang, P.; Luo, G.Q.; Chen, F.; Shen, Q.; Zhang, L.M.; Lavernia, E.J. Effect of plasma activated sintering parameters on microstructure and mechanical properties of Al-7075/B_4C composites. *J. Alloy. Compd.* **2014**, *615*, 276–282. [CrossRef]
12. Ipek, R. Adhesive wear behaviour of B_4C and SiC reinforced 4147 Al matrix composites (Al/B_4C-Al/SiC). *J. Mater. Process. Technol.* **2005**, *162*, 71–75. [CrossRef]
13. Dou, Y.H.; Liu, Y.; Liu, Y.B.; Xiong, Z.P.; Xia, Q.B. Friction and wear behaviors of B_4C/6061Al composite. *Mater. Des.* **2014**, *60*, 669–677. [CrossRef]
14. Hu, S.W.; Zhao, Y.G.; Wang, Z.; Li, Y.G.; Jiang, Q.C. Fabrication of in situ TiC locally reinforced manganese steel matrix composite via combustion synthesis during casting. *Mater. Des.* **2013**, *44*, 340–345. [CrossRef]
15. Zhou, Z.S.; Wu, G.H.; Jiang, L.T.; Li, R.F.; Xu, Z.G. Analysis of morphology and microstructure of B_4C/2024Al composites after 7.62 mm ballistic impact. *Mater. Des.* **2014**, *63*, 658–663.

16. Sarikaya, O.; Anik, S.; Aslanlar, S.; Okumus, S.C.; Celik, E. Al-Si/B_4C composite coatings on Al-Si substrate by plasma spray technique. *Mater. Des.* **2007**, *28*, 2443–2449. [CrossRef]
17. Wu, F.; Lu, J. Applications and the properties of boron carbide ceramic material. *J. Wuyi Univ.* **2002**, *3*, 45–49.
18. Kang, P.C.; Cao, Z.W.; Wu, G.H.; Zhang, J.H.; Wei, D.J.; Lin, L.T. Phase identification of Al-B_4C ceramic composites synthesized by reaction hot-press sintering. *Int. J. Refract. Met. Hard Mater.* **2010**, *28*, 297–300. [CrossRef]
19. Arslan, G.; Kara, F.; Turan, S. Quantitative X-ray diffraction analysis of reactive infiltrated boron carbide-aluminium composites. *J. Eur. Ceram. Soc.* **2003**, *23*, 1243–1255. [CrossRef]
20. Halverson, D.C.; Pyzik, A.J.; Aksay, I.A.; Snowden, W.E. Processing of boron carbide-aluminum composites. *J. Am. Ceram. Soc.* **1989**, *72*, 775–780.